Year: 2006

Properties of galaxy groups in the Sloan Digital Sky Survey - II. Active galactic nucleus feedback and star formation truncation

Weinmann, S M ; Van Den Bosch, F C ; Yang, X ; Mo, H J ; Croton, D J ; Moore, B

Abstract: Successfully reproducing the galaxy luminosity function (LF) and the bimodality in the galaxy distribution requires a mechanism that can truncate star formation in massive haloes. Current models of galaxy formation consider two such truncation mechanisms: strangulation, which acts on satellite galaxies, and active galactic nucleus (AGN) feedback, which predominantly affects central galaxies. The efficiencies of these processes set the blue fraction of galaxies, fblue(L, M), as a function of galaxy luminosity, L, and halo mass, M. In this paper, we use a galaxy group catalogue extracted from the Sloan Digital Sky Survey (SDSS) to determine fblue(L, M). To demonstrate the potential power of these data as a benchmark for galaxy formation models, we compare the results to the semi-analytical model for galaxy formation of Croton et al. Although this model accurately fits the global statistics of the galaxy population, as well as the shape of the conditional LF, there are significant discrepancies when the blue fraction of galaxies as a function of mass and luminosity is compared between the observations and the model. In particular, the model predicts (i) too many faint satellites in massive haloes, (ii) a blue fraction of satellites that is much too low, and (iii) a blue fraction of centrals that is too high and with an inverted luminosity dependence. In the same order, we argue that these discrepancies owe to (i) the neglect of tidal stripping in the semi-analytical model, (ii) the oversimplified treatment of strangulation, and (iii) improper modelling of dust extinction and/or AGN feedback. The data presented here will prove useful to test and calibrate future models of galaxy formation and, in particular, to discriminate between various models for AGN feedback and other star formation truncation mechanisms

Properties of galaxy groups in the Sloan Digital Sky Survey – II. Active galactic nucleus feedback and star formation truncation

Simone M. Weinmann,[1]⋆ Frank C. van den Bosch,[2] Xiaohu Yang,[3] H. J. Mo,[2] Darren J. Croton[5] and Ben Moore[1]

[1]*Institute for Theoretical Physics, University of Zurich, CH-8057 Zurich, Switzerland*
[2]*Max-Planck-Institute for Astronomy, Königstuhl 17, D-69117 Heidelberg, Germany*
[3]*Shanghai Astronomical Observatory; the Partner Group of MPA, Nandan Road 80, Shanghai 200030, China*
[4]*Department of Astronomy, University of Massachusetts, 710 North Pleasant Street, Amherst, MA 01003-9305, USA*
[5]*Department of Astronomy, University of California at Berkeley, Mail Code 3411, Berkeley, CA 94720, USA*

ABSTRACT

Successfully reproducing the galaxy luminosity function (LF) and the bimodality in the galaxy distribution requires a mechanism that can truncate star formation in massive haloes. Current models of galaxy formation consider two such truncation mechanisms: strangulation, which acts on satellite galaxies, and active galactic nucleus (AGN) feedback, which predominantly affects central galaxies. The efficiencies of these processes set the blue fraction of galaxies, $f_{\mathrm{blue}}(L, M)$, as a function of galaxy luminosity, L, and halo mass, M. In this paper, we use a galaxy group catalogue extracted from the Sloan Digital Sky Survey (SDSS) to determine $f_{\mathrm{blue}}(L, M)$. To demonstrate the potential power of these data as a benchmark for galaxy formation models, we compare the results to the semi-analytical model for galaxy formation of Croton et al. Although this model accurately fits the *global* statistics of the galaxy population, as well as the shape of the conditional LF, there are significant discrepancies when the blue fraction of galaxies as a function of mass and luminosity is compared between the observations and the model. In particular, the model predicts (i) too many faint satellites in massive haloes, (ii) a blue fraction of satellites that is much too low, and (iii) a blue fraction of centrals that is too high and with an inverted luminosity dependence. In the same order, we argue that these discrepancies owe to (i) the neglect of tidal stripping in the semi-analytical model, (ii) the oversimplified treatment of strangulation, and (iii) improper modelling of dust extinction and/or AGN feedback. The data presented here will prove useful to test and calibrate future models of galaxy formation and, in particular, to discriminate between various models for AGN feedback and other star formation truncation mechanisms.

Key words: methods: statistical – galaxies: evolution – galaxies: formation – galaxies: general – galaxies: statistics.

1 INTRODUCTION

One of the most challenging outstanding problems in galaxy formation is to explain the detailed shape of the galaxy luminosity function (LF). In particular, the relatively shallow faint-end slope and the exponential cut-off at the bright end of the LF have proven difficult to explain (e.g. White & Frenk 1991; Benson et al. 2003). In the traditional scenario for galaxy formation, it is envisioned that lower cooling efficiencies in massive galaxies would explain the exponential tail of the LF (Rees & Ostriker 1977; Silk 1977; White & Rees 1978), while supernova feedback is typically invoked to reduce the star formation efficiency in low-mass haloes (Larson 1974; White

& Rees 1978; Dekel & Silk 1986). Although the latter can indeed be tuned to reproduce the faint-end slope of the galaxy LF, it worsens the problems at the bright end. As nicely demonstrated by Benson et al. (2003), supernova feedback causes a drastic increase of the amount of diffuse hot gas that remains in larger haloes. This gas is able to cool on to the central galaxies in these haloes, producing too many bright galaxies. In addition, this causes the bright model galaxies to have relatively young stellar populations, in disagreement with observations (e.g. Kauffmann & Charlot 1998; Heavens et al. 2004; Thomas et al. 2005). What is needed is a mechanism that can truncate the star formation in these massive, central galaxies at relatively late times.

Star formation truncation is also the main mechanism that is thought to underlie the bimodality of galaxy properties. The local population of galaxies consists roughly of two types: red galaxies,

---

⋆E-mail: weinmann@physik.unizh.ch

which reveal an early-type morphology and which have very little or no ongoing star formation, and blue galaxies with active star formation and a late-type morphology (e.g. Strateva et al. 2001; Blanton et al. 2003a; Kauffmann et al. 2003, 2004; Baldry et al. 2004; Balogh et al. 2004a,b; Brinchmann et al. 2004). Although a non-negligible fraction of red galaxies are clearly edge-on disc galaxies that owe their red colour to an enhanced extinction, the most pronounced distinction between 'red-sequence' and 'blue-sequence' galaxies is their current star formation rate. Since only relatively small amounts of ongoing star formation tend to make a galaxy appear 'blue', the colour bimodality basically reflects star formation truncation: red-sequence galaxies have their star formation truncated, while blue-sequence galaxies are still forming stars today.

Semi-analytical models for galaxy formation consider a number of mechanisms that can prevent, delay or truncate star formation. In low-mass haloes, one typically invokes reionization and supernova feedback in order to suppress or truncate star formation. In haloes with $M \gtrsim 10^{12}~h^{-1}$ M$_\odot$, on which we will focus in this paper, two additional truncation effects are considered. The first one, called strangulation, only affects satellite galaxies. As soon as a dark matter halo is accreted by a larger halo, its central galaxy becomes a satellite galaxy. It is often assumed that this accretion process causes the satellite galaxy to be stripped of its hot gas reservoir. Consequently, after a delay time in which the galaxy consumes (a part of) its cold gas, star formation is truncated, and the satellite galaxy becomes red (Larson, Tinsley & Caldwell 1980; Balogh, Navarro & Morris 2000). Ram-pressure stripping (Gunn & Gott 1972) may shorten the time-delay, by also stripping the satellite of its cold gas reservoir, but since the time-scale for strangulation is already relatively short, the addition of ram-pressure stripping does not have a large impact. Virtually all semi-analytical models of galaxy formation, starting with Kauffmann, White & Guiderdoni (1993), have taken this strangulation mechanism into account. In fact, it is the main mechanism that causes red-sequence model galaxies to preferentially reside in overdense regions such as groups and clusters of galaxies, in good agreement with observations (e.g. Oemler 1974; Dressler 1980; Balogh et al. 2004b; Hogg et al. 2004; Weinmann et al. 2006).

The second star formation truncation mechanism that operates in massive haloes is feedback from active galactic nuclei (AGN), which predominantly affects central galaxies. Although the potential importance of AGN feedback has long been recognized (e.g. Tabor & Binney 1993; Ciotti & Ostriker 1997), it only recently has been given serious consideration in galaxy formation models. This has largely been motivated by X-ray observations which reveal that AGN can indeed impact the hot intergalactic medium (IGM) of galaxy clusters (e.g. Fabian et al. 2003; McNamara et al. 2005). Numerous recent studies have demonstrated that the inclusion of AGN feedback in galaxy formation models can help to explain the bright end exponential cut-off of the galaxy LF (e.g. Granato et al. 2004; Bower et al. 2006; Cattaneo et al. 2006a; Croton et al. 2006; Sijacki & Springel 2006) and the fact that the most-massive galaxies contain the oldest stars (Scannapieco, Silk & Bouwens 2005; Bower et al. 2006; Croton et al. 2006).

Despite these successes, we are still far from a proper understanding of how AGN feedback may establish an equilibrium state where it can efficiently suppress star formation in the centres of massive haloes. In the studies mentioned above, AGN feedback is typically modelled using oversimplified, heuristic scaling relations, often based on very different views of how AGN feedback might operate. In particular, it is still unclear which mode of AGN activity is most important for the star formation truncation discussed above; the

merger-induced 'quasar mode' which leads to an initial starburst followed by a quenching of star formation, or the 'radio mode', which is caused by continual and quiescent accretion of hot gas on to the central supermassive black hole. Hopkins et al. (2006) have suggested that merger-induced AGN activity (the 'quasar mode') is responsible for the transition from blue, star forming to red, passive galaxies. Springel, Di Matteo & Hernquist (2005a), Menci et al. (2005) and Kang, Jing & Silk (2006) have shown that this 'quasar-mode' feedback can indeed terminate star formation and expel the gas from the centre of the galaxy, once the supermassive black holes become sufficiently massive. On the other hand, Croton et al. (2006), Bower et al. (2006), Cattaneo et al. (2006a), Nusser, Silk & Babul (2006) and Sijacki & Springel (2006) have argued that the 'radio mode' of AGN activity (or AGN feedback operating in quasi-hydrostatically cooling haloes) is the main mechanism to truncate star formation in massive galaxies. How exactly this radio mode feedback operates, however, is still unclear, as is evident from the fact that the aforementioned studies all use very different formulations.

All these different AGN feedback models mainly differ in the way in which the feedback efficiency scales with halo mass and with galaxy properties such as black hole mass and gas mass fraction. Since AGN feedback causes star formation truncation, one way to discriminate between these various models is therefore to investigate the relative fractions of blue and red galaxies as a function of halo mass and galaxy properties. Such a study will also help to improve our understanding of strangulation, the star formation truncation mechanism for satellites. Although strangulation is typically modelled as being independent of halo mass, one might argue that the ability of a host halo to strip a subhalo of its hot gas reservoir depends on the presence and density of the hot corona of the host halo which, in turn, may well be mass-dependent. Again, knowledge of the fractions of blue and red (satellite) galaxies as a function of halo mass should allow us to discriminate between these different possibilities.

Nowadays, with large galaxy surveys, such as the Two-Degree Field Galaxy Redshift Survey (Colless et al. 2001) and the Sloan Digital Sky Survey (SDSS; York et al. 2000), the number of galaxies is sufficiently large that, in principle, one could accurately measure the red and blue fractions as a function of various variables. In this paper, we use our SDSS group catalogue, presented in Weinmann et al. (2006, hereafter Paper I), to compute the fractions of blue and red galaxies as a function of both halo mass and galaxy luminosity. To emphasize the potential constraining power of these data, we compare our results to the semi-analytical galaxy formation model of Croton et al. (2006), which includes both strangulation and 'radio-mode' AGN feedback. We show that although this model accurately fits the galaxy LF, the colour-bimodality, and many other *global* statistics of the galaxy population, it fails dramatically when it comes down to the blue fraction of galaxies as a function of halo mass and luminosity. We argue that this has its origin in the way that strangulation and AGN feedback have been incorporated and we briefly discuss possible modifications. The aim of this paper, however, is not to present a new, improved model for star formation truncation, but merely to present observational constraints that will hopefully prove useful in discriminating between the various models.

This paper is organized as follows. Section 2 describes our SDSS group catalogue, which we compare to a similar group catalogue extracted from the semi-analytical model of Croton et al. (2006) described in Section 3. The actual comparison is presented in Section 4, whereas Section 5 discusses the possible implications for galaxy formation models. We summarize our results in Section 6.

2 THE SLOAN DIGITAL SKY SURVEY GROUP CATALOGUE

2.1 Data

The SDSS (York et al. 2000) is a joint, five passband (*u*, *g*, *r*, *i* and *z*) imaging and medium-resolution ($R \sim 1800$) spectroscopic survey. In this paper, we focus on the subset of galaxies that are in the New York University Value-Added Galaxy Catalogue (NYU-VAGC) based on the SDSS Data Release 2 (Blanton et al. 2005). This NYU-VAGC is based on an independent, significantly improved data reduction. From this catalogue, we select all galaxies with an extinction-corrected apparent magnitude brighter than $r = 17.77$, with redshifts in the range $0.01 \leqslant z \leqslant 0.20$, and with a redshift completeness $\mathcal{C} > 0.7$. This leaves a grand total of 184 425 galaxies. In what follows, we use M_r and $^{0.1}M_r$ to indicate the absolute magnitude in the *r* band, *k*-corrected to $z = 0$ and 0.1, respectively. All *k*-corrections are based on the model described in Blanton et al. (2003b).

We split the galaxies into 'red' and 'blue' subsamples using a magnitude-dependent cut, which roughly follows the observed bimodality scale in the colour–magnitude relation

$$^{0.1}(g - r)_{\text{cut}} = 0.7 - 0.032 \left[^{0.1}M_r + 16.5 \right] \tag{1}$$

(cf. Paper I). In what follows, we refer to galaxies that are redder and bluer than $^{0.1}(g - r)_{\text{cut}}$ as 'red' and 'blue' galaxies, respectively.

2.2 The group-finding algorithm

Our working definition of a galaxy group is an ensemble of galaxies that reside in the same dark matter parent halo; galaxies that reside in subhaloes are considered to be group members that belong to the parent halo in which the subhalo is located. We have used the halo-based group finder developed by Yang et al. (2005a, hereafter YMBJ) in order to group the galaxies in the above-mentioned galaxy catalogue. This particular group finder has been optimized to group galaxies according to their common dark matter halo, and has been thoroughly tested with mock galaxy redshift surveys. In brief, the method works as follows. First, potential group centres are identified using a Friends-Of-Friends (FOF) algorithm or an isolation criterion. Next, the total group luminosity is estimated which is converted into an estimate for the group mass using an assumed mass-to-light ratio (*M/L*). From this mass estimate, the radius and velocity dispersion of the corresponding dark matter halo are estimated using the virial equations which, in turn, are used to select group members in redshift space. This method is iterated until group memberships converge. A more detailed description is given in appendix A of Paper I.

In YMBJ, the performance of this group finder has been tested in terms of completeness of true members and contamination by interlopers, using detailed mock galaxy redshift surveys. The average completeness of individual groups was found to be $\sim$90 per cent, with only $\sim$20 per cent interlopers. Furthermore, the resulting group catalogue is insensitive to the initial assumption regarding the *M/L*s, and the group finder is more successful than the conventional FOF method (e.g. Huchra & Geller 1982; Ramella, Geller & Huchra 1989; Merchán & Zandivarez 2002; Eke et al. 2004; Berlind et al. 2006) in associating galaxies according to their common dark matter haloes.

2.3 Estimating group masses

Following YMBJ, we use the group luminosity to assign masses to our groups. The motivation behind this is that one naturally expects the group luminosity to be strongly correlated with halo mass (albeit with a certain amount of scatter). Since the group luminosity is dominated by the brightest members, which are exactly the ones that can be observed in a flux-limited survey like the SDSS, the determination of the (total) group luminosity is more robust than that of the group's velocity dispersion, especially when the number of group members is small (see appendix B in Paper I).

Clearly, because of the flux limit of the SDSS, two identical groups observed at different redshifts will have a different L_{group}, defined as the summed luminosity of all its identified members. To circumvent this bias, we first need to bring the group luminosities to a common scale. A nearby group selected in an apparent magnitude limited survey should contain all of its members down to a faint luminosity. We can therefore use these nearby groups to determine the relation between the group luminosity obtained using only galaxies above a bright luminosity limit and that obtained using galaxies above a fainter luminosity limit. Assuming that this relation is redshift-independent, one can correct the luminosity of a high-*z* group, where only the brightest members are observed, to an empirically normalized luminosity scale.

As a common luminosity scale, we use $L_{19.5}$, defined as the luminosity of all group members brighter than $^{0.1}M_r = -19.5 + 5 \log h$. To calibrate the relation between L_{group} and $L_{19.5}$, we first select all groups with $z \leqslant 0.09$, which corresponds to the redshift for which a galaxy with $^{0.1}M_r = -19.5 + 5 \log h$ has an apparent magnitude that is equal to the magnitude limit of the survey. For groups with $z > 0.09$, we use this 'local' calibration between L_{group} and $L_{19.5}$ to estimate the latter. Detailed tests have shown that the resulting group luminosities are significantly more reliable than those in which the correction for missing members is based on the assumption of a universal LF (see YMBJ for details).

The final step is to obtain an estimate of the group (halo) mass from $L_{19.5}$. This is done using the assumption that there is a one-to-one relation between $L_{19.5}$ and halo mass. For each group, we determine the number density of all groups brighter (in terms of $L_{19.5}$) than the group in consideration. Using the halo mass function corresponding to a Λ cold dark matter (ΛCDM) concordance cosmology with $\Omega_{\text{m}} = 0.3$, $\Omega_{\Lambda} = 0.7$, $h = H_0/(100 \,\text{km s}^{-1} \,\text{Mpc}^{-1}) = 0.7$ and $\sigma_8 = 0.9$, we then find the mass for which the more-massive haloes have the same number density. Although the masses thus derived depend on cosmology, it is straightforward to convert the masses derived here to any other cosmology.

Finally, we note that not all groups can have a halo mass assigned to them. First of all, the mass estimator described above does not work for groups in which all members are fainter than $^{0.1}M_r = -19.5 + 5 \log h$. Secondly, the combination of $L_{19.5}$ and redshift may be such that we know that the halo catalogue is incomplete, which means that there is a significant number of groups at this redshift with the same $L_{19.5}$ but for which the individual galaxies are too faint to be detected. Since our mass assignment is based on the assumption of completeness, any group beyond the completeness redshift corresponding to its $L_{19.5}$ is not assigned a halo mass (see Yang et al. 2005b for details).

2.4 The SDSS group catalogue

Applying our group finder to the sample of SDSS galaxies described in Section 2.1 yields a group catalogue of 53 229 systems with an estimated mass. These groups contain a total of 92 315 galaxies. The majority of the groups (37 216 systems) contain only a single member, while there are 9220 binary systems, 3073 triplet systems, and

3720 systems with four members or more (see Paper I for details).[1] In what follows, we refer to the brightest galaxy in each group as the 'central' galaxy, while all others are termed 'satellites'.

3 THE SEMI-ANALYTIC MODEL

The semi-analytic model (SAM) to which we compare the SDSS group catalogue discussed above is based on an output of the Millennium Run *N*-body simulation (Springel et al. 2005b) and is described in detail in Croton et al. (2006, hereafter C06). The simulation is based on the cosmological parameters $\Omega_m = 0.25$, $\Omega_\Lambda = 0.75$, $\Omega_b = 0.045$, $h = 0.73$ and $\sigma_8 = 0.9$ and has a volume of $0.125\,h^{-3}$ Gpc^3. Dark matter haloes are identified with an FOF group finder, and subsequently populated with galaxies following the semi-analytical model described in C06.

One of the relative novelties of this SAM is the inclusion of 'radio-mode' feedback from AGN that lie at the centre of a halo with a static corona of hot gas. As shown in C06, this feedback mode suppresses the cooling flow in massive haloes at relatively late times which, in turn, yields luminosities, colours and stellar ages for massive galaxies in better agreement with observations. In particular, the inclusion of the radio-mode AGN feedback can explain the exponential cut-off at the bright end of the galaxy LF, and the fact that the most-massive galaxies are red and consist of old stellar populations (see De Lucia et al. 2006 for details). The model also predicts star formation histories, cold gas mass fractions and metallicities that are all in good agreement with observations. The model even predicts a Tully–Fisher zero-point that matches the data, as long as the rotation velocity of a disc galaxy is equal to the maximum circular velocity of the dark matter halo (however, the rather unorthodox implication of this assumption is that the dark matter halo would actually expand rather than contract during galaxy formation, see Dutton et al. 2006). Since the halo masses M assigned to our SDSS galaxy groups are obtained by matching the abundances to the halo mass function, these are to be interpreted as the masses inside a radius with an overdensity of 180. As shown by Jenkins et al. (2001), for this definition of halo mass the analytical halo mass function of Sheth, Mo & Tormen (2001) used here is in good agreement with the halo mass function obtained from numerical simulations. The halo masses in the C06 catalogue, however, are defined as the masses inside a radius with a mean density that is 200 times the critical density, which we denote by M_{200}. In order to convert M_{200} to M, we assume that dark matter haloes follow an NFW density distribution (Navarro, Frenk & White 1997). Using the relation between halo mass and halo concentration of Eke, Navarro & Steinmetz (2001), we find that the relation between M and M_{200} is well fitted by

$$\frac{M_{200}}{M} = 0.745 - 0.0006\,[\log(M_{200}) - 7.0]^{2.45}. \tag{2}$$

In what follows, we only consider the galaxies with $M_r \leqslant -16.72$, which reflects the magnitude completeness limit of the SAM, yielding a total of approximately nine million model galaxies. The main information used in this paper is the *r*- and *g*-band magnitudes of these galaxies, and the mass M of the halo in which they reside. For comparison with the SDSS, we also compute the *g*- and *r*-band magnitudes *k*-corrected to $z = 0.1$, using

$$^{0.1}g = g + 0.3113 + 0.4620\,(g - r - 0.6102), \tag{3}$$

and

$$^{0.1}r = g - 0.4075 - 0.8577\,(g - r - 0.6102) \tag{4}$$

(Blanton et al. 2003b).[2]

As we will see below, despite the AGN feedback the SAM still contains a significant number of very bright and blue galaxies that are not present in the SDSS. As mentioned in C06, these are mainly ultraluminous infrared galaxy (ULIRG)-type starbursts for which the dust treatment of the model is inadequate; with a more proper dust model, these galaxies would be much more extincted, making them both fainter and redder. In order to suppress the impact of these galaxies on our SAM–SDSS comparison, we remove all galaxies with $(g - r) < 0$ from both the SAM and the SDSS. In the case of the SAM this only affects 0.5 per cent of all galaxies, whereas in the case of the SDSS, this fraction is completely negligible.

We split the SAM model galaxies into 'red' and 'blue' subsamples using the same magnitude-dependent colour-cut as for the SDSS, given by equation (1). In addition, we discriminate between 'central' galaxies, defined as the galaxy in a halo that is closest to the halo centre, and 'satellite' galaxies. This differs from the definition used for the group catalogues, where the central galaxy is defined as the brightest group member. However, 97.5 per cent of all central galaxies in the SAM are also the brightest galaxy in their halo, virtually independent of halo mass. We have verified that defining central galaxies in the SAM as the brightest halo members instead does not have a significant impact on any of our results.

3.1 Constructing a SAM redshift survey

In order to be able to compare the SAM to the SDSS results, we need to mimic the construction of a galaxy redshift survey. We do so using the following steps. First, we construct a large virtual universe by replicating the periodic simulation box in a stack of $2 \times 2 \times 2$ boxes. This is required in order to be able to probe out to sufficiently high redshifts. Next, we compute the redshift and apparent magnitude of each galaxy as seen by a virtual observer located in a corner of this virtual universe (who can thus see $\pi/2$ sr of 'sky'). We mimic the selection criteria of the SDSS discussed in Section 2.1 by only selecting those galaxies with $0.01 < z < 0.2$ and with $r < 17.77$. This leaves us with a grand total of 428 013 model galaxies. In what follows, we refer to this sample as the 'SAM redshift survey' (SAM-RS).

Fig. 1 compares a number of statistics of these galaxies with those from the SDSS. The upper panels plot the distribution of absolute magnitudes, $^{0.1}M_r$, and their contribution due to red (dotted curves) and blue (dashed curves) galaxies. The agreement is very satisfactory, consistent with the fact that the SAM matches the observed LFs (see C06). The second row of panels indicate the colour distributions. Once again, the agreement is reasonable, although the bimodality in the SAM-RS seems somewhat more pronounced than in the SDSS, with a somewhat narrower 'red peak'. Nevertheless, with blue fractions of 48 and 46 per cent in the SDSS and SAM-RS, respectively, the overall agreement is very satisfactory.

In the third row of panels, we 'compare' two different morphology indicators. For the SDSS galaxies, we plot the distribution of the concentration c, defined as the ratio between the radii that contain 90 and 50 per cent of the Petrosian flux. For the SAM model

---

[1] This SDSS group catalogue is publicly available at http://www.astro.umass.edu/~xhyang/Group.html.

[2] These filter transformations are taken from a manuscript in preparation by Michael Blanton and Sam Roweis, available at http://cosmo.nyu.edu/blanton/kcorrect.
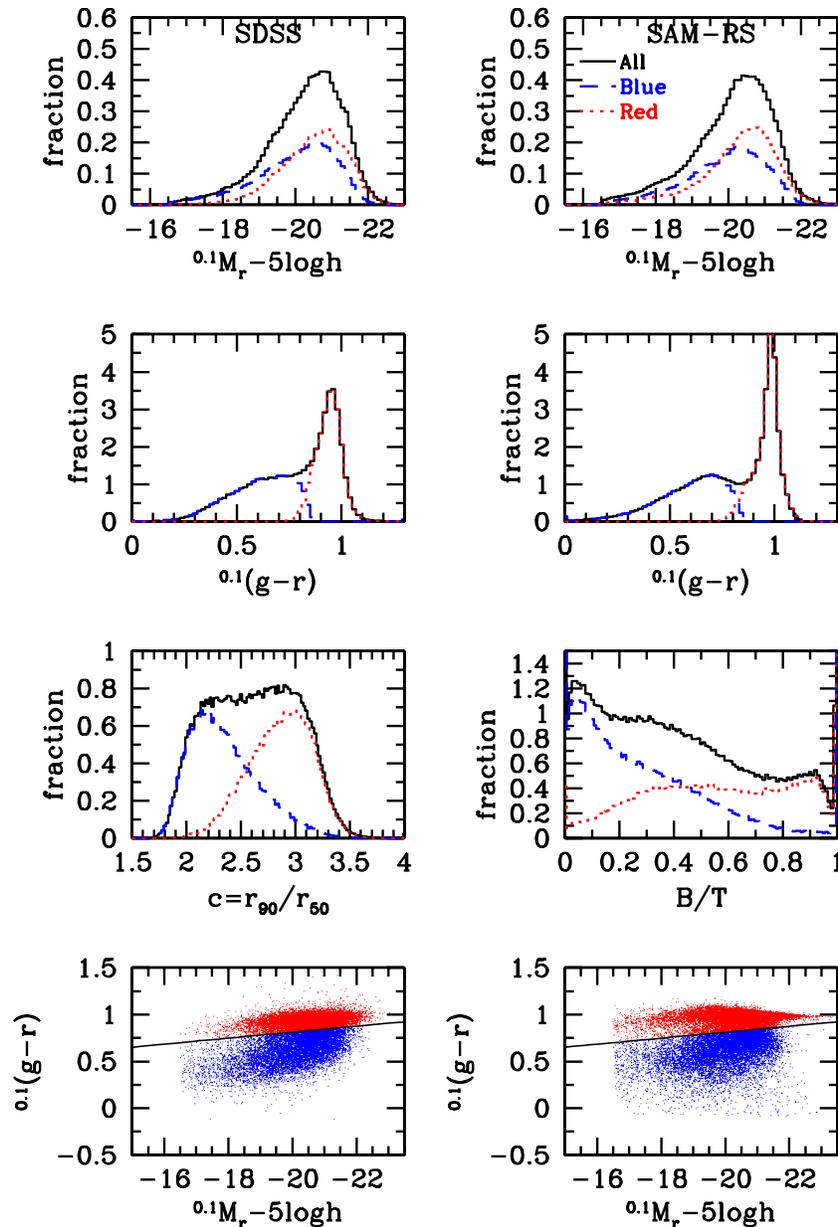
Figure 1. A comparison of global statistics of the SAM-RS (right-hand panels) with the SDSS (left-hand panels). The panels in the first and second row show histograms of absolute $^{0.1}$ r-band magnitude and $^{0.1}$ $(g - r)$ colour for both redshift surveys. The contributions from blue and red galaxies are indicated by the dashed and dotted lines, respectively. Note the good agreement between the SDSS and the SAM-RS. The panels in the third row show histograms of morphological parameters. In the case of the SDSS, we plot the distribution of the concentration parameter, c, defined as the ratio of the radii containing 90 and 50 per cent of the petrosian flux. In the case of the SAM-RS, we plot the distribution of the B/T instead. Although these cannot be compared directly, in general a more concentrated galaxy (higher c) will also have a larger B/T. Again, the contributions from red and blue galaxies are indicated. Finally, the fourth row of panels show the colour–magnitude relations. The solid line indicates the bimodality scale given by equation (1), which we use to split the population of galaxies in red and blue subpopulations.

galaxies, we plot the distribution of the bulge-to-total stellar mass ratio (B/T) instead. Typically, a galaxy with a large B/T will also have a high concentration parameter. For both c and B/T, there is a very significant overlap of red and blue galaxies. Therefore, our split in red and blue galaxies does not necessarily correspond to a morphological split in early- and late-type galaxies, respectively, even though both are clearly correlated (see fig. 1 in Paper I).

Finally, the lower panels of Fig. 1 show scatter plots of the colour–magnitude relations. The solid line corresponds to the bimodality scale given by equation (1). Again, there is reason-

able overall agreement between the SAM-RS and the SDSS, although there are more galaxies with very blue colours in the SAM-RS, especially at the bright end. Recall that galaxies with $(g - r) < 0$ have already been excluded from these plots. As mentioned before, these bright, blue galaxies would appear significantly fainter and redder with proper dust modelling. Another apparent discrepancy concerns the red sequence, which at the bright end appears significantly tighter for the SAM than for the SDSS, which is also apparent from the histograms in the second row of panels.

To summarize, despite some small discrepancies, the global, statistical properties of the SAM model galaxies are in good agreement with the SDSS. However, this does not mean that the SAM also predicts the correct statistics *as a function of halo mass*. This is clearly a much tighter constraint for the model and, as we argued in Section 1, may provide useful insights regarding the halo-mass dependence of various physical processes.

3.2 Construction of the SAM group catalogue

The main goal of this paper is to compare the fractions of red and blue galaxies as a function of both halo mass and luminosity in the SAM with those obtained from our SDSS group catalogue. In principle, we could do so by comparing our SDSS group results directly with the SAM. However, our group finder and, in particular, the algorithm used to assign the masses, is not perfect. Hence, it is unclear whether any discrepancy between the SDSS group catalogue and the SAM reflects an artefact of the group finder, or whether there is a true difference in the halo occupation statistics of the SDSS and SAM. To circumvent this problem, we use the SAM-RS described above to construct a 'SAM group catalogue' (SAM-GC) using exactly the same group finder and mass assignment algorithm as those applied to the SDSS. By comparing this SAM-GC with the SDSS group catalogue, we significantly reduce the impact of possible inaccuracies related to the group finder, making the comparison more fair.

Application of our group finder to the SAM-RS described above yields 98 130 groups with an assigned mass, which host a total of 206 076 galaxies. This amounts to an average of 2.10 members per group, which is significantly higher than that for the SDSS, where the groups with an assigned mass have on average 1.73 members. However, the SDSS is not complete; in fact, the average completeness of our SDSS sample is 0.88, which largely explains the difference in the mean number of members per group. Another reason for this discrepancy is that, as we will see, massive haloes in the SAM contain too many faint satellites compared to the SDSS.

The fraction of blue galaxies in the SAM-GC is only 29 per cent. Comparing this to the fraction of 46 per cent of blue galaxies in the SAM-RS indicates that a red galaxy is much more likely to be associated with a group than a blue galaxy. At first sight, this seems a logical consequence of the fact that (i) our group catalogue is limited to relatively massive haloes with $M \gtrsim 5 \times 10^{11} \, h^{-1} \, M_\odot$, and (ii) low-mass haloes are more likely to host blue galaxies (see e.g. Paper I). However, the application of the group finder to the SDSS only reduces the fraction of blue galaxies from 48 to 41 per cent. This reduction is much less severe than that for the SAM. This is the first indication that the SAM and SDSS do not agree well when it comes down to details regarding the distribution of red and blue galaxies (see Section 4.2 below).

Since the SAM contains the full halo occupation information, we can check whether our group finder has assigned the correct galaxies to the same group, and whether the assigned mass is in agreement with the true halo mass. We have performed a large number of tests to investigate how well the group finder allows us to recover the true relations between galaxies and their dark matter haloes. Several of these tests have been described in detail in YMBJ and Yang et al. (2005b), and show that the average occupation statistics of dark matter haloes are accurately recovered. However, higher-order moments of the occupation statistics, such as the scatter around a mean relation, are typically severely underestimated by the group catalogue, due to the fact that we assume a one-to-one relation between halo mass and halo luminosity (with zero scatter) when assigning masses to our groups. As an illustration of the accuracy of our group finder,
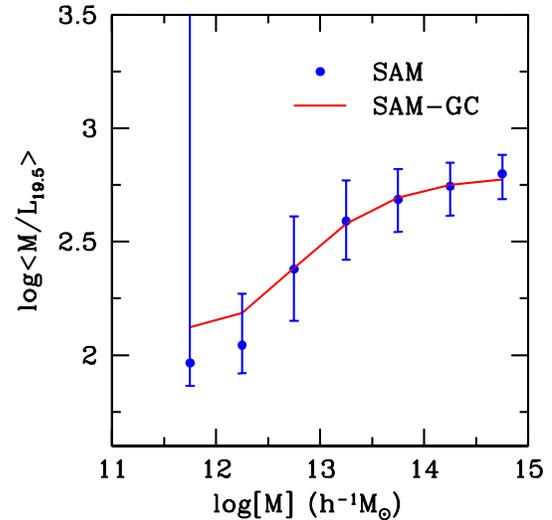

Figure 2. The average mass-to-light ratio, $\langle M/L_{19.5} \rangle$, as a function of halo (group) mass. Here $L_{19.5}$ is the total luminosity of all galaxies in a halo with $^{0.1}M_r - 5 \log h \leqslant -19.5$. The filled circles with error bars (indicating the 68 per cent confidence level) show the results obtained from the SAM directly, using the original halo masses and halo membership. The solid line shows the $\langle M/L_{19.5} \rangle$ as obtained from the SAM group catalogue, and is thus based on the assigned group masses and the assigned group memberships. The agreement with the true $\langle M/L_{19.5} \rangle$ is excellent, indicating that our group finder allows an accurate recovery of the average relation between mass and light.

Fig. 2 plots the average M/L of the dark matter haloes in the SAM (symbols with error bars). Here M is the halo mass defined according to equation (2), and L is the total luminosity in the $^{0.1}r$ band of all galaxies in that halo with $^{0.1}M_r - 5 \log h \leqslant -19.5$. The solid line in Fig. 2 shows the average M/Ls obtained from the SAM-GC, which agree extremely well with the true $\langle M/L \rangle_M$. This demonstrates that our group finder can accurately recover the average relation between mass and light.

In what follows, whenever we present any result obtained from the SAM-GC, we will also present the same results extracted directly from the SAM (using the true halo masses and the true halo memberships). A comparison among these results safeguards against potential problems with the group finder.

4 GALAXY ECOLOGY

4.1 Conditional luminosity functions

We start our SAM–SDSS comparison by focusing on the conditional luminosity function (CLF), $\Phi(L \mid M)$, which specifies the average number of galaxies of luminosity L that reside in a halo of mass M (van den Bosch, Yang & Mo 2003; Yang, Mo & van den Bosch 2003). The upper panels of Fig. 3 show the CLFs obtained from the SDSS group catalogue. Results are shown for four different mass bins, as indicated at the top of each column. Note that these masses are the assigned group masses. The dotted (blue) and dashed (red) lines indicate the contributions from the satellite and central galaxies, respectively. The distribution of central galaxies is well approximated by a log-normal distribution, consistent with previous findings (Yang et al. 2005b; Zheng et al. 2005). The panels in the middle row of Fig. 3 show the CLFs obtained directly from the SAM; here the masses are the true halo masses, and the true halo
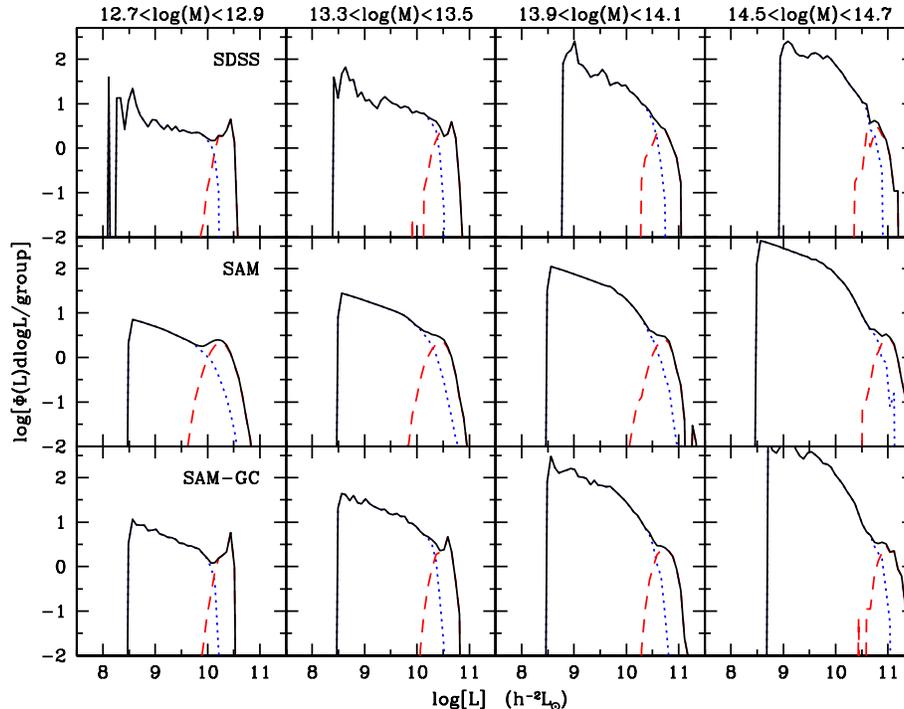
Figure 3. The CLF obtained from the SDSS group catalogue (upper panel) from the SAM directly, using true halo masses and true halo members (middle panel) and from the SAM group catalogue, using assigned group masses and assigned memberships (lower panels). Results are shown for four different mass bins (masses in h^{-1} M$_\odot$), as indicated at the top of each column. Luminosities are in the $^{0.1}$ r band. The dotted (blue) line marks the contribution from the satellite galaxies; the dashed (red) line marks the contribution from the central galaxies.

members are used to construct the CLFs. The overall agreement with the CLFs extracted from the SDSS group catalogue is very satisfactory, although the width of the CLF for central galaxies is significantly broader in the SAM than in the SDSS. To allow for a more meaningful comparison, the lower panels of Fig. 3 plot the CLFs obtained from the SAM-GC. The first thing to note is that the widths of the CLFs of the central galaxies are now in much better agreement with those of the SDSS; apparently, the group finder artificially 'narrows' the scatter in the relation between the halo mass and the luminosity of the central galaxy. This simply owes to the fact that we use the group luminosity to determine the group mass. Other than that, the agreement between the CLFs obtained from the SAM-GC, and those extracted directly from the SAM is very good, indicating that our group finder allows an accurate recovery of the true $\Phi(L\,|\,M)$ (see also tests in Yang et al. 2005b).

Except for the highest-mass bin, the CLFs extracted from the SDSS and the SAM group catalogues are in good agreement with each other, indicating that the SAM not only fits the galaxy LF, but also does so as a function of halo mass. However, at the massive end the SAM predicts significantly more relatively faint galaxies in massive haloes than observed. In the highest-mass bin shown, the SAM overpredicts the number of faint satellites with $L = 3 \times 10^9\,h^{-2}$ L$_\odot$ by a factor of ∼2. Since these are virtually all red, early-type galaxies (see below), this suggests that the SAM overpredicts the number density of faint, red galaxies. Indeed, as already shown in C06, the SAM overpredicts the LF of red galaxies at the faint end. The analysis here suggests that this largely owes to an overabundance of satellite galaxies in massive haloes with $M \gtrsim 3 \times 10^{14}\,h^{-1}$ M$_\odot$.

We emphasize that this discrepancy is not due to the fact that we have ignored fibre collisions in the SDSS. Since the spectroscopic

fibres of the SDSS have a minimum angular separation of 55 arcsec, the spectroscopic catalogue suffers from an incompleteness on small angular scales. This will impact on the multiplicity function of the groups in our catalogue. However, as shown by Berlind et al. (2006), the effect is relatively small, typically reducing the multiplicity of groups by ∼10 per cent, which is negligible compared to the factor of 2 eluded to above. We have performed tests using a version of the NYU-VAGC which gives each galaxy missing from the redshift survey because of fibre-collisions the redshift of its nearest neighbour. To prevent bright foreground galaxies from being artificially shifted to high redshift and thus contaminating the results, each of these galaxies also is assigned the magnitude, but not the colour, of its nearest neighbour galaxy. We have constructed a new group catalogue with this extended sample, and find no qualitative changes in any of our results.

4.2 Blue fraction as a function of luminosity

The dotted line in the upper left-hand panel of Fig. 4 shows the fraction of blue galaxies, $f_{\rm blue}$, in the SDSS as a function of luminosity. Here, all 184 425 galaxies in our SDSS sample defined in Section 2.1 are used. As is well known, the fraction of blue galaxies decreases drastically with increasing luminosity, dropping from ∼95 per cent at $^{0.1}M_r - 5\log h = -16$ to $\lesssim 5$ per cent for galaxies with $^{0.1}M_r - 5\log h < -22.5$. The dashed line in the lower left-hand panel shows the blue fraction for the 428 013 model galaxies in the SAM-RS. Although this blue fraction also reveals an overall decrease with increasing luminosity, there are two marked differences with respect to the SDSS. First of all, at the bright end there is a sudden upturn in $f_{\rm blue}$; galaxies with $^{0.1}M_r - 5\log h \simeq -23$ have a blue fraction of ∼26 ± 6 per cent, compared to zero per cent in the SDSS (note
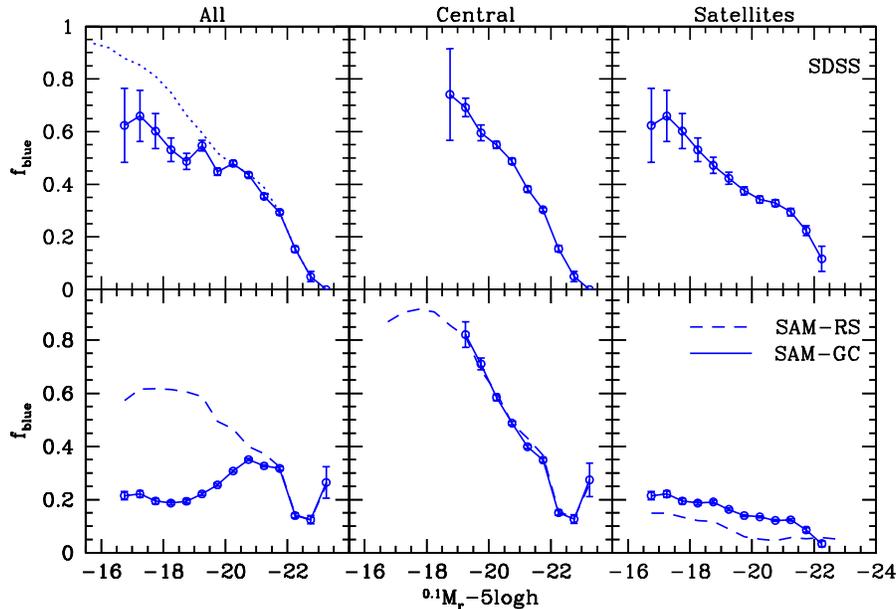
Figure 4. The luminosity dependence of blue galaxy fractions. From the left- to right-hand side, the panels show the blue fractions of all galaxies (centrals plus satellites), central galaxies, and satellite galaxies. The top panels show the results from the SDSS group catalogue (open circles with Poissonian error bars). The dotted line in the top left-hand panel shows the results obtained from the full SDSS, including those galaxies that were not assigned to a galaxy group by the group finder. The bottom panels show the results from the SAM of C06. Results are shown for both the SAM-RS (dashed lines) and the SAM-GC (open circles with Poissonian error bars). See Section 4.2 for a detailed discussion.

though that there are only eight SDSS galaxies in this luminosity bin). As already mentioned in Section 3, these bright blue galaxies in the SAM are ULIRGs for which the dust modelling is inadequate (cf. lower panels of Fig. 1). The second discrepancy between the SAM-RS and the SDSS is more important; at the faint end the blue fraction in the SAM-RS never exceeds 62 per cent, and is therewith much lower than the blue fraction of faint SDSS galaxies. Consistent with what we inferred above from the CLFs, this indicates that the SAM severely overpredicts the fraction of faint, red galaxies.

To investigate whether this mainly concerns central galaxies, satellite galaxies, or both, we now resort to the group catalogues extracted from the SDSS and SAM. The open circles with error bars, connected by the solid lines, indicate the blue fractions of galaxies that make it into the group catalogue. Comparing these for the SDSS to those obtained from the full sample (dotted lines), we see that the blue fraction has become somewhat lower at the faint end. We can understand this by looking at the blue fractions of central galaxies (upper middle panel) and satellite galaxies (upper right-hand panel). This shows that both blue fractions decrease with increasing luminosity, but that the luminosity dependence is more pronounced for the centrals. Since the galaxies that do *not* make it into the group catalogue are mainly isolated, and thus central, galaxies that live in haloes below the mass limit of the group catalogue, these are mainly blue. This explains why the fraction of faint blue galaxies is lower in the group catalogue than in the full redshift catalogue.

In the SAM, the group selection also causes a drop of the blue fraction of faint galaxies, but of a much larger amplitude. In fact, the fraction of 'group' galaxies with $-16 > M_{b_J} - 5 \log h > -18$ is ~20 per cent in the SAM, compared to ~60 per cent in the SDSS. The reason for this discrepancy is largely due to the satellite galaxies: as shown in the lower right-hand panel, the blue fraction of satellite galaxies in the SAM is much too low, especially at the faint end. In the case of the central galaxies (middle panels), the agreement between the SAM and the SDSS is much better, especially for

centrals with $M_{b_J} - 5 \log h \simeq -21$. However, at the faint and bright ends, the SAM significantly overpredicts the blue fractions by ~15 and ~25 per cent, respectively.

The dashed lines in the lower middle and lower right-hand panels show the blue fractions of centrals and satellites of *all* galaxies in the SAM-RS (including those that are not in the group catalogue). This shows that the group finder very accurately recovers the blue fraction of central galaxies, but slightly overpredicts that of satellites. This owes to the interlopers (group members that do not actually belong to the same halo), which tend to be isolated, central galaxies in low-mass haloes, and which are thus preferentially blue. The contamination, however, is sufficiently small that it does not significantly affect any of our results.

In summary, although the SAM matches the overall blue fraction of galaxies almost exactly (see Section 3.1), when split according to luminosity or according to centrals and satellites, there are very significant differences between the SAM and SDSS. The SAM overpredicts the blue fraction of central galaxies at both the bright and the faint end of the distribution, and dramatically underpredicts the blue fraction of (faint) satellite galaxies. In particular, the SAM predicts that virtually all ($\gtrsim 85$ per cent) satellite galaxies are red, whereas the SDSS indicates that the fraction of red satellites decreases from ~90 per cent at $^{0.1}M_r = -22 + 5 \log h$ to ~40 per cent at $^{0.1}M_r = -17 + 5 \log h$. This suggests shortcomings for the star formation truncation mechanisms in the SAM: apparently the treatment of strangulation is too efficient, while the model for AGN feedback is not efficient enough (see Section 5 for a more detailed discussion).

4.3 Blue fraction as a function of halo mass

We now turn to the mass dependence of f_{blue}. We split the SDSS and SAM group catalogues in six logarithmic mass bins and determine how the blue fractions in each of these bins depend on luminosity.
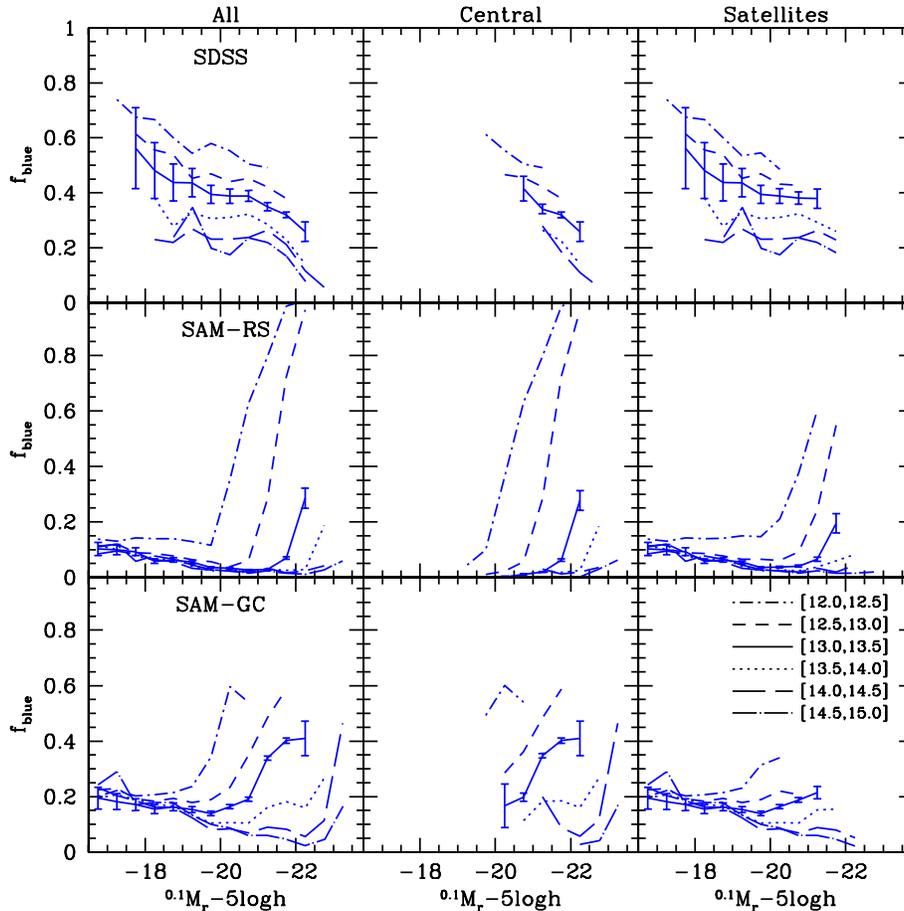
Figure 5. Blue galaxy fractions as a function of absolute magnitude in the $^{0.1}r$ band. Results are shown for all galaxies (left-hand panels), central galaxies (middle panels) and satellite galaxies (right-hand panels), and for six different mass bins as indicated [the values in square brackets indicate the range of log $(M/h^{-1}\ \mathrm{M_{\odot}})$]. Results are only shown for mass–luminosity bins that contain at least 50 galaxies in total, and for clarity (Poissonian) error bars are only shown for one mass bin. From top to bottom panel, results are shown for the SDSS group catalogue, the SAM redshift survey (SAM-RS), and the SAM group catalogue (SAM-GC). Note the poor agreement between SDSS and SAM-GC, indicating that the SAM is not correctly treating the physics responsible for determining whether a galaxy is red or blue. See Section 4.3 for a detailed discussion.

For each bin in mass and luminosity, the blue fraction is defined as the total number of blue galaxies in that bin, divided by the total number of galaxies in that bin (i.e. we do not average the blue fraction over individual groups or haloes).

The results for the SDSS group catalogue are shown in the upper panels of Fig. 5 and are listed in tabular form in Appendix A. The upper left-hand panel shows the result for all galaxies (centrals plus satellites). In each mass bin, the blue fraction decreases with increasing luminosity, but only very mildly. In fact, over the magnitude range $-19 \gtrsim {}^{0.1}M_r - 5\log h \gtrsim -21.5$ the luminosity dependence is remarkably weak, for all six mass bins. At fixed luminosity, however, there is a clear mass dependence, with the blue fraction decreasing with increasing halo mass. Over the range $10^{12} \lesssim M \lesssim 10^{15}\ h^{-1}\,\mathrm{M_{\odot}}$, the blue fraction changes by $\sim$30 per cent, at all luminosities. This indicates that the colour of a galaxy is more strongly determined by the mass of the halo in which it resides than by its own luminosity (cf. Yang et al. 2005b; Paper I). Consequently, the strong luminosity dependence of f_{blue} seen in Fig. 4 is mainly a reflection of the fact that more-luminous galaxies typically reside in more-massive haloes. Note that some earlier work (e.g. Balogh et al. 2004b; Tanaka et al. 2004) has found no correlation between galaxy properties and halo velocity dispersion. However, as shown in Paper I this is most likely due to the smaller sample size and the

fact that using velocity dispersion as a mass estimator tends to smear out the mass dependence.

The upper middle panel shows the blue fractions of central galaxies. Note that at a given halo mass, there is only a relatively small dynamic range of luminosities over which we can measure $f_{\mathrm{blue}}(L)$. Nevertheless, at a given halo mass there is a clear indication that the blue fraction decreases with increasing luminosity. At the same time, at a given luminosity the blue fraction also decreases with increasing halo mass. Finally, the upper right-hand panel shows the results for the satellite galaxies in the SDSS group catalogue, which look similar to those for the full sample of galaxies shown in the upper left-hand panel.

The middle and lower rows of panels in Fig. 5 show the results obtained from the SAM-RS and SAM-GC, respectively. In the former, no group finder has been applied, and the mass binning is according to the true halo masses of the galaxies. A comparison with the results obtained from the SAM group catalogue is therefore indicative of the accuracy with which our group finder allows a recovery of the true underlying $f_{\mathrm{blue}}(L, M)$. A number of differences are clearly apparent, which mainly owe to the impact of interlopers and, more importantly, to errors in the assigned group masses. Since the true $f_{\mathrm{blue}}(L, M)$ has extremely steep gradients in both L and M, even small errors in any of these quantities can have a significant impact

on the blue fraction obtained from the group catalogue. This mainly causes errors in the *absolute* values of $f_{\text{blue}}(L, M)$. However, the *relative* relations of $f_{\text{blue}}(L \,|\, M)$ and $f_{\text{blue}}(M \,|\, L)$ are well recovered. Note that the blue fraction of central galaxies with $^{0.1}M_r - 5 \log h = -19.5$ is less than 10 per cent for all mass bins shown. Yet, as can be seen from Fig. 4, the blue fraction of central galaxies in the group catalogue with that luminosity is ∼80 per cent. This indicates that virtually all blue centrals with $^{0.1}M_r - 5 \log h \leqslant -19.5$ reside in haloes with $M < 10^{12} \, h^{-1} \, \text{M}_\odot$.

Comparing the $f_{\text{blue}}(L, M)$ obtained from the SAM-GC with those obtained from the SDSS, one notes immediately that they have very little in common. Probably the most dramatic difference between the SDSS and the SAM-GC concerns the blue fraction of satellite galaxies (shown in the panels on the right-hand side), which is much too low in the SAM-GC, especially for faint galaxies and for low-mass haloes. A comparison with the SAM-RS results shows that this discrepancy cannot be attributed to artefacts of the group finder. In addition, the SAM-GC predicts that the blue fraction of central galaxies increases with increasing luminosity, opposite to what is seen in the SDSS (middle panels). This effect is most severe for haloes with masses $M < 10^{13} \, h^{-1} \, \text{M}_\odot$. These two problems conspire to produce a blue fraction of the full galaxy population (centrals and satellites) in the SAM-GC which is very different from the SDSS (left hand panels), both quantitatively (mainly because of the too low number of blue satellites) and qualititatively (mainly because of the reversed relation between luminosity and the blue fraction of central galaxies).

We are thus led to conclude that although the SAM reproduces the overall blue fraction (when integrated over all galaxies), when it comes to $f_{\text{blue}}(L, M)$, there are dramatic differences between model and data. Note that the SAM of C06 fits the overall LF and even yields CLFs, that is, LFs as a function of halo mass, whose shapes are in remarkably good agreement with the SDSS data. This suggests that one of the main problems for the SAM is the treatment of the physics responsible for determining whether a galaxy is red or blue. This includes not only the star formation truncation mechanisms, such as strangulation and AGN feedback, but also the treatment of dust extinction. In the next section, we present a more detailed discussion of the possible implications.

5 DISCUSSION

The above analysis of the fractions of blue galaxies as a function of halo mass and luminosity has revealed several problems for the SAM of C06. In the following, we discuss the possible implications for galaxy formation models.

5.1 Tidal stripping

The first problem concerns the abundance of satellite galaxies. As shown in Section 4.1, the SAM overpredicts the number of faint satellite galaxies in massive haloes by up to a factor of ∼2. Most likely, this indicates that the luminosity evolution of the satellites is not properly accounted for. Satellite galaxies can become fainter due to star formation truncation followed by passive evolution, or due to tidal stripping of their stellar mass. Since most of the satellite galaxies in the SAM are already red, they cannot become much fainter than they already are for their given stellar mass. In other words, there is little to gain from adding physical processes that may speed up the star formation truncation, such as ram-pressure stripping. In fact, this will only increase the fraction of red satellites, which is already much too large. The most plausible explanation for the overabundance of satellite galaxies is the neglect of tidal

stripping. It is well known that the tides in massive haloes can easily strip satellite galaxies and their dark matter haloes of large fractions of their mass. This is supported by the detection of intracluster light (e.g. Bernstein et al. 1995; Gonzalez et al. 2000) due to a diffuse population of intergalactic stars. Most likely, these stars, which contribute around 10 per cent of the total cluster light (Zibetti et al. 2005), have been tidally stripped off from satellite galaxies.

Formalisms to describe tidal stripping in the presence of dynamical friction in a background potential have been developed by, among others, Taylor & Babul (2001, 2004) and Zentner & Bullock (2003). As shown in Benson et al. (2002), including such a formalism in semi-analytical models significantly reduces the abundance of satellite galaxies. Furthermore, since tidal stripping predominantly affects satellites with small pericentric radii, which are typically redder (blue galaxies have only recently been accreted by the halo, and have not yet experienced much dynamical friction), tidal stripping may also reduce the red fraction of satellites and thus help towards solving the problem with the red fractions of satellites being too large.

5.2 Strangulation

The second problem for the SAM of C06 is that the fraction of blue satellite galaxies is much too low, especially for faint galaxies and in low-mass haloes. This suggests that 'strangulation', as incorporated in the SAM, is much too efficient. In virtually all semi-analytical models, strangulation is included and modelled in the same way: as soon as a galaxy becomes a satellite galaxy, its hot gas reservoir is 'stripped' off (i.e. the hot gas that belonged to the satellite galaxy is added to the hot gas reservoir of the central galaxy). Consequently, after a delay time in which the new satellite galaxy consumes (a part of) its cold gas, its star formation is truncated. The results presented here suggest that this formulation is too crude, as it predicts a blue satellite fraction that is much too low.[3] In particular, strangulation is modelled without any explicit halo mass dependence, which explains why the blue fraction of satellite galaxies in the SAM is virtually independent of halo mass. In the SDSS, however, the blue satellite fraction decreases with increasing halo mass, suggesting a clear mass scaling of the strangulation efficiency. The physical mechanisms thought to be responsible for the removal of the satellite's hot gas reservoir are tides and ram-pressure stripping. The latter requires that the parent halo has a sufficiently dense hot corona. Since this requirement is more likely to be fulfilled for more-massive haloes, which in general have a larger fraction of hot gas, one actually expects that the strangulation efficiency increases with increasing halo mass. Indeed, using numerical simulations, Bekki, Couch & Shioya (2002) found that strangulation is significantly more effective in massive galaxy clusters than in lower mass groups. It remains to be seen whether a simple scaling along these lines can bring the red and blue fractions of satellite galaxies in SAMs in better agreement with the SDSS data presented here.

Interestingly, in a comparison of semi-analytical models and hydrodynamical smoothed particle hydrodynamics (SPH) simulations of galaxy formation, Zheng et al. (2005) have shown that the latter predicts that haloes with $10^{12} \lesssim M \lesssim 10^{13} \; \text{M}_\odot$ have a significantly higher fraction of young satellites (similar to the blue satellites discussed here) than SAMs, in much better agreement with the

---

[3] Note that the SAM of C06, as most other SAMS, does not even account for ram-pressure stripping, which will only shorten the truncation time, thus decreasing the blue satellite fraction.

SDSS results presented here (see their fig. 4). Similarly, Cattaneo et al. (2006b) found that their SAM produces too few blue satellite galaxies compared to their SPH simulation. Since these SPH simulations follow the actual hydrodynamical processes leading to strangulation, this indeed suggests that a more realistic treatment of strangulation in the SAMs may solve the problem with the colours of satellite galaxies. SPH simulations such as those described in Zheng et al. (2005) and Cattaneo et al. (2006b) may prove useful in calibrating such a new and improved strangulation model. In fact, hydrodynamical simulations using grid-based schemes may be even better suited to study gas-stripping processes than SPH, especially since they seem to be able to more accurately capture Kelvin–Helmholtz instabilities (Agertz et al., in preparation). Ram-pressure stripping, on the other hand, can be modelled equally well with both simulation schemes (Abadi, Moore & Bower 1999; Quilis, Moore & Bower 2000).

5.3 Dust extinction and AGN feedback

The SAM also has problems with the blue fractions of central galaxies, which are too high, especially at the bright and faint ends. In addition, for a given halo mass, the blue fraction of central galaxies increases with luminosity, contrary to what is seen in the SDSS. Which aspect(s) of the semi-analytical model are responsible for these problems is not entirely clear. They can indicate a problem with the modelling of dust extinction, a problem with the treatment of AGN feedback, or both. The former is almost certainly responsible for the overproduction of bright and blue centrals. As already discussed in C06, this population of galaxies is reminiscent of the ULIRG population, for which the oversimplified treatment of the dust extinction is certainly inadequate: real starbursts are likely to be accompanied by additional extinction which would make these galaxies both fainter and redder. This would help to suppress the strong increase in f_{blue} with increasing luminosity, though it remains to be seen whether it can result in a blue fraction that decreases with increasing luminosity, as observed. Furthermore, in order to suppress the impact of these starbursting model galaxies on the comparison presented here, we already removed all galaxies with $(g - r) < 0$ from the SAM. Despite this, however, the SAM still significantly overpredicts the fraction of blue centrals with $^{0.1}M_r - 5 \log h \simeq -23$. Although improper dust modelling is likely to be the cause for this discrepancy, it remains to be seen whether this can also explain the overprediction (by ~ 15 per cent) of the blue fraction of *faint* centrals.

Alternatively, the blue fractions of central galaxies may be modified by changing the AGN feedback description. As discussed in the Introduction section, it is still largely unknown how AGN impact on their surroundings, and thus feed back on the process of galaxy formation. It should therefore not come as a surprise if the parametrization of C06 is not entirely correct or complete. Other semi-analytical models of AGN feedback do not parametrize the energy feedback rate as a function of black hole mass and halo mass as in C06, but assume that AGN feedback is self-regulating under certain conditions, and either becomes effective above a critical halo mass (Cattaneo et al. 2006a) or is switched on if the Eddington luminosity of the black hole is large enough (Bower et al. 2006). It is unclear whether these different prescriptions can alleviate the problems presented here. The purpose of this paper, however, is not to find an improved formulation of AGN feedback. Rather, we have presented data, in the form of blue galaxy fractions as a function of both halo mass and luminosity, which we believe to be useful in discriminating between different AGN feedback models. Future SAMs can test and/or calibrate their particular parametrizations against these data.

6 CONCLUSIONS

It has become clear that a successful reproduction of the galaxy LF, and of the bimodality in the galaxy distribution, requires a mechanism that can truncate the star formation in massive galaxies at relatively late epochs. At the same time, the fact that red, passive galaxies preferentially reside in overdense regions, such as clusters and groups of galaxies, suggests that star formation truncation acts preferentially in massive haloes. Current models consider two such truncation mechanisms: strangulation, which acts on satellite galaxies, and AGN feedback, which predominantly affects central galaxies.

Typically, galaxy formation models are tuned to reproduce the *global* properties of the galaxy distribution, such as the LF and the total fraction of blue and red galaxies. However, even when two models predict exactly the same global statistics, their statistics as a function of halo mass may be very different. The latter is clearly more constraining for the model, and furthermore, holds important information regarding the mass dependence of the various physical mechanisms associated with galaxy formation. In particular, since star formation truncation causes a galaxy to become red, the relative fractions of red and blue galaxies as a function of halo mass hold important clues regarding the halo mass dependence of the efficiencies of AGN feedback and strangulation.

To provide a test-bed for models of galaxy formation, we have used a galaxy group catalogue extracted from the SDSS for which we have computed the fraction of blue and red galaxies as a function of both galaxy luminosity and group (halo) mass. To illustrate the potential constraining power of these data, we have compared these fractions to those in the semi-analytical model for galaxy formation of C06, which includes both 'radio-mode' AGN feedback and strangulation. To allow for a fair comparison between the SDSS group catalogue and the SAM, not influenced by potential inaccuracies associated with the group finder (i.e. interlopers, incompleteness, errors in assigned group mass), we have applied the same group finder over a mock redshift survey constructed from the SAM. The $f_{blue}(L, M)$ obtained from this SAM group catalogue is in fair agreement with the true $f_{blue}(L, M)$ obtained directly from the SAM, indicating that our group finder allows a reliable recovery of the blue fraction as a function of both galaxy luminosity and halo mass. Although interlopers and errors in the group masses may cause some errors in the absolute values of $f_{blue}(L, M)$, the relative scalings of $f_{blue}(L \mid M)$ and $f_{blue}(M \mid L)$ are well recovered.

Although the SAM fits the overall LF, reproduces the overall colour distribution of the SDSS galaxies, and even predicts a CLF whose shape is in excellent agreement with the data, its prediction of $f_{blue}(L, M)$ is in poor agreement with the SDSS data. In particular, we have identified four problems as listed below.

(i) In massive haloes, the abundance of faint satellite galaxies is too high by up to a factor of ~ 2.

(ii) The fraction of blue satellite galaxies is much too low, especially for faint galaxies and in low-mass haloes.

(iii) The fraction of blue central galaxies is too high, especially at the bright and faint ends.

(iv) For a given halo mass, the blue fraction of central galaxies increases with luminosity, contrary to what is seen in the SDSS.

The first of these problems is likely to owe to the fact that the SAM does not model the tidal stripping of the stellar mass of

the satellite galaxies as they orbit the parent halo. As shown in Benson et al. (2002), inclusion of this effect significantly reduces the abundance of satellite galaxies at a fixed luminosity. The second problem is most likely due to an oversimplification of the treatment of strangulation. In the SAM, strangulation occurs instantaneously, independent of halo mass. However, based on the SDSS data, we have argued that the strangulation efficiency has to scale with halo mass, such that more-massive haloes strangulate their satellites on a shorter time-scale. The physical motivation for such a scaling is that the ram-pressure stripping of the hot gas reservoir of newly accreted satellites requires the parent halo to have a sufficiently dense corona of hot gas. Since the fraction of hot gas is typically an increasing function of halo mass, this may introduce a mass dependence in the strangulation efficiency as required. Indeed, hydrodynamical SPH simulations, which automatically take this into account, seem to predict blue satellite fractions that are significantly higher than those in the semi-analytical models (Zheng et al. 2005; Cattaneo et al. 2006b). Finally, the third and fourth problem listed above, both of which concern central galaxies, are likely to reflect shortcomings of the modelling of dust extinction and/or AGN feedback.

In summary, galaxy formation models are often tested and calibrated against global properties of the observed galaxy distribution. Recently, with the inclusion of AGN feedback, numerous studies have claimed success in reproducing these global statistics, even though very different formulations for the various physical processes have been used. In order to discriminate between these models, more specific data are required. In this paper, we have presented the fractions of blue and red galaxies as a function of luminosity, halo mass, and separately for central and satellite galaxies. Clearly, these data are far more constraining, and thus more challenging, than the global fractions of red and blue galaxies, or the overall LF. We have shown that indeed these data provide valuable new insights into the physics of galaxy formation, and we hope that they will provide a useful test-bed for future models of galaxy formation.

REFERENCES

Abadi M. G., Moore B., Bower R. G., 1999, MNRAS, 308, 947
Baldry I. K., Glazebrook K., Brinkmann J., Ivezić Ž., Lupton R. H., Nichol R. C., Szalay A. S., 2004, ApJ, 600, 681
Balogh M. L., Navarro J. F., Morris S. L., 2000, ApJ, 540, 113
Balogh M. L. et al., 2004a, MNRAS, 348, 1355
Balogh M. L., Baldry I. K., Nichol R., Miller C., Bower R., Glazebrook K., 2004b, ApJ, 615, L101
Bekki K., Couch W. J., Shioya Y., 2002, ApJ, 651, 657
Benson A. J., Lacey C. G., Baugh C. M., Cole S., Frenk C. S., 2002, MNRAS, 333, 156
Benson A. J., Bower R. G., Frenk C. S., Lacey C. G., Baugh C. M., Cole S., 2003, ApJ, 599, 38
Berlind A. A. et al., 2006, preprint (astro-ph/0601346)
Bernstein G. M., Nichol R. C., Tyson J. A., Ulmer M. P., Wittman D., 1995, AJ, 110 1507
Blanton M. R. et al., 2003a, ApJ, 594, 186
Blanton M. R. et al., 2003b, AJ, 125, 2348
Blanton M. R. et al., 2005, AJ, 129, 2562
Bower R. G., Benson A. J., Malbon R., Helly J. C., Frenk C. S., Baugh C. M., Cole S., Lacey C. G., 2006, MNRAS, 370, 645
Brinchmann J., Charlot S., White S. D. M., Tremonti C., Kauffmann G., Heckman T., Brinkmann J., 2004, MNRAS, 353, 713
Cattaneo A., Dekel A., Devriendt J., Guiderdoni B., Blaizot J., 2006a, MNRAS, 370, 1651
Cattaneo A. et al., 2006b, preprint (astro-ph/0605750)
Ciotti L., Ostriker J. P., 1997, ApJ, 487, L105
Colless M. et al., 2001, MNRAS, 328, 1039
Croton D. J. et al., 2006, MNRAS, 365, 11 (C06)
Dekel A., Silk J., 1986, ApJ, 303, 39
De Lucia G., Springel V., White S. D. M., Croton D., Kauffmann G., 2006, MNRAS, 366, 499
Dressler A., 1980, ApJ, 236, 351
Dutton A. A., van den Bosch F. C., Dekel A., Courteau S., 2006, MNRAS submitted (astro-ph/0604553)
Eke V. R., Navarro J. F., Steinmetz M., 2001, ApJ, 554, 114
Eke V. R. et al. (the 2dFGS team), 2004, MNRAS, 348, 866
Fabian A. C., Sanders J. S., Crawford C. S., Cornelice C. J., Gallagher J. S., Wyse R. F. G., 2003, MNRAS, 344, L43
Gonzalez A. H., Zabludoff A. I., Zaritsky D., Dalcanton J. J., 2000, ApJ, 536, 561
Granato G. L., De Zotti G., Silva L., Bressan A., Danese L., 2004, MNRAS, 600, 580
Gunn J. E., Gott J. R., 1972, ApJ, 176, 1
Heavens A., Panter B., Jimenez R., Dunlop J., 2004, Nat, 428, 625
Hogg D. W. et al., 2004, ApJ, 601, L29
Hopkins P. F., Hernquist L., Cox T. J., Di Matteo T., Robertson B., Springel V., 2006, ApJS, 163, 1
Huchra J. P., Geller M. J., 1982, ApJ, 257, 423
Jenkins A., Frenk C. S., White S. D. M., Colberg J. M., Cole S., Evrard A. E., Couchman H. M. P., Yoshida N., 2001, MNRAS, 321, 372
Kang X., Jing Y. P., Silk J., 2006, ApJ, 648, 820
Kauffmann G., Charlot S., 1998, MNRAS, 294, 705
Kauffmann G., White S. D. M., Guiderdoni B., 1993, MNRAS, 264, 201
Kauffmann G. et al., 2003, MNRAS, 341, 33
Kauffmann G., White S. D. M., Heckman T. M., Ménard B. J., Charlot S., Tremonti C., Brinkmann J., 2004, MNRAS, 353, 713
Larson R. B., 1974, MNRAS, 169, 229
Larson R. B., Tinsley B. M., Caldwell C. N., 1980, ApJ, 237, 692
McNamara B. R., Nulsen P. E. J., Wise M. W., Rafferty D. A., Carilli C., Sarazin C. L., Blanton E. L., 2005, Nat, 433, 45
Menci N., Fontana A., Giallongo E., Salimbeni S., 2005, ApJ, 632, 49

Merchán M., Zandivarez A., 2002, MNRAS, 335, 216

Navarro J. F., Frenk C. S., White S. D. M., 1997, ApJ, 490, 493

Nusser A., Silk J., Babul A., 2006, preprint (astro-ph/0602566)

Oemler A., 1974, ApJ, 194, 1

Quilis V., Moore B., Bower R., 2000, Sci, 288, 1617

Ramella M., Geller M. J., Huchra J. P., 1989, ApJ, 344, 57

Rees M. J., Ostriker J. P., 1977, MNRAS, 179, 541

Scannapieco E., Silk J., Bouwens R., 2005, ApJ, 635, L13

Sheth R. K., Mo H. J., Tormen G., 2001, MNRAS, 323, 1

Sijacki D., Springel V., 2006, MNRAS, 366, 397

Silk J., 1977, ApJ, 211, 638

Springel V., Di Matteo T., Hernquist L., 2005a, MNRAS, 361, 776

Springel V., White S. D. M., Jenkins A. et al., 2005b, Nat, 435, 629

Strateva I. et al., 2001, ApJ, 122, 1861

Tabor G., Binney J., 1993, MNRAS, 263, 323

Tanaka M., Goto T., Okamura S., Shimasaku K., Brinkman J., 2004, AJ, 128, 2677

Taylor J. E., Babul A., 2001, ApJ, 559, 716

Taylor J. E., Babul A., 2004, MNRAS, 348, 811

Thomas D., Maraston C., Bender R., de Oliveira C. M., 2005, ApJ, 621, 673

van den Bosch F. C., Yang X., Mo H. J., 2003, MNRAS, 340, 771

Weinmann S. M., van den Bosch F. C., Yang X., Mo H. J., 2006, MNRAS, 366, 2 (Paper I)

White S. D. M., Rees M. J., 1978, MNRAS, 183, 341

White S. D. M., Frenk C. S., 1991, ApJ, 379, 52

Yang X., Mo H. J., van den Bosch F. C., 2003, MNRAS, 339, 1057

Yang X., Mo H. J., van den Bosch F. C., Jing Y. P., 2005a, MNRAS, 356, 1293 (YMBJ)

Yang X., Mo H. J., Jing Y. P., van den Bosch F. C., 2005b, MNRAS, 358, 217

York D. G. et al., 2000, AJ, 120, 1579

Zentner A. R., Bullock J. S., 2003, ApJ, 598, 49

Zheng Z. et al., 2005, ApJ, 633, 791

Zibetti S., White S. D. M., Schneider D. P., Brinkmann J., 2005, MNRAS, 358, 949

APPENDIX A: BLUE GALAXY FRACTIONS IN THE SDSS

The following three tables list the fraction of blue galaxies for all galaxies (Table A1), for satellite galaxies (Table A2), and for central galaxies (Table A3), as obtained from our SDSS group catalogue. The columns correspond to different bins in log (M), with M in units of h^{-1} M$_\odot$, as indicated at the top in square brackets. The rows correspond to different magnitude bins $(^{0.1}M_r - 5 \log h)$, as indicated at the left-hand side in square brackets. Each entry lists the blue fraction plus, in brackets, the total number of galaxies (all, satellite or central) in that bin. As in Fig. 5, only entries with at least 50 galaxies are indicated.

Table A1. Blue fractions of all galaxies.

	[12, 12.5]	[12.5, 13]	[13, 13.5]	[13.5, 14]	[14, 14.5]	[14.5, 15]
[−17, −17.5]	0.74 (69)	–	–	–	–	–
[−17.5, −18]	0.68 (108)	0.61 (114)	0.56 (80)	–	–	–
[−18, −18.5]	0.67 (186)	0.56 (189)	0.48 (133)	0.38 (84)	0.23 (74)	–
[−18.5, −19]	0.60 (308)	0.54 (343)	0.44 (265)	0.28 (213)	0.22 (96)	0.24 (67)
[−19, −19.5]	0.54 (461)	0.45 (489)	0.44 (449)	0.33 (392)	0.27 (246)	0.35 (98)
[−19.5, −20]	0.58 (909)	0.47 (1113)	0.39 (987)	0.30 (878)	0.23 (654)	0.20 (208)
[−20, −20.5]	0.55 (9366)	0.44 (1673)	0.39 (1445)	0.31 (1172)	0.23 (771)	0.17 (296)
[−20.5, −21]	0.50 (7890)	0.45 (3181)	0.39 (2556)	0.32 (1673)	0.24 (1058)	0.23 (380)
[−21, −21.5]	0.49 (61)	0.42 (4752)	0.35 (3657)	0.28 (2164)	0.26 (1068)	0.22 (371)
[−21.5, −22]	–	0.38 (956)	0.32 (7327)	0.23 (2231)	0.21 (1001)	0.17 (326)
[−22, −22.5]	–	–	0.26 (464)	0.14 (1181)	0.11 (476)	0.08 (143)
[−22.5, −23]	–	–	–	–	0.06 (108)	–

Table A2. Blue fractions of satellite galaxies.

	[12, 12.5]	[12.5, 13]	[13, 13.5]	[13.5, 14]	[14, 14.5]	[14.5, 15]
[−17, −17.5]	0.74 (69)	–	–	–	–	–
[−17.5, −18]	0.68 (108)	0.61 (114)	0.56 (80)	–	–	–
[−18, −18.5]	0.67 (186)	0.56 (189)	0.48 (133)	0.38 (84)	0.23 (74)	–
[−18.5, −19]	0.60 (308)	0.54 (343)	0.44 (265)	0.28 (213)	0.22 (96)	0.24 (67)
[−19, −19.5]	0.53 (449)	0.45 (489)	0.44 (449)	0.33 (392)	0.27 (246)	0.35 (98)
[−19.5, −20]	0.54 (437)	0.47 (1101)	0.39 (987)	0.30 (878)	0.23 (654)	0.20 (208)
[−20, −20.5]	0.48 (66)	0.43 (1235)	0.39 (1425)	0.31 (1172)	0.23 (771)	0.17 (296)
[−20.5, −21]	–	0.43 (389)	0.38 (2005)	0.32 (1624)	0.24 (1057)	0.23 (380)
[−21, −21.5]	–	–	0.38 (810)	0.29 (1568)	0.26 (1000)	0.22 (368)
[−21.5, −22]	–	–	–	0.26 (408)	0.23 (621)	0.18 (283)

Table A3. Blue fractions of central galaxies.

	[12, 12.5]	[12.5, 13]	[13, 13.5]	[13.5, 14]	[14, 14.5]	[14.5, 15]
[−19.5, −20]	0.61 (472)	–	–	–	–	-
[−20, −20.5]	0.55 (9300)	0.47 (438)	–	–	–	–
[−20.5, −21]	0.51 (7890)	0.46 (2792)	0.42 (551)	–	–	–
[−21, −21.5]	0.49 (61)	0.42 (4752)	0.34 (2847)	0.26 (596)	0.28 (68)	–
[−21.5, −22]	–	0.38 (956)	0.32 (7324)	0.22 (1823)	0.18 (380)	–
[−22, −22.5]	–	–	0.26 (464)	0.14 (1178)	0.11 (444)	0.07 (95)
[−22.5, −23]	–	–	–	–	0.06 (108)	–

This paper has been typeset from a TEX/LATEX file prepared by the author.